British Journal of Pharmacology

British Journal of Pharmacology (2017) **174** 2636–2651 2636

RESEARCH PAPER

# Vitamin D receptor agonists regulate ocular developmental angiogenesis and modulate expression of dre-miR-21 and VEGF

**Correspondence** Breandán N. Kennedy, UCD School of Biomolecular and Biomedical Science, UCD Conway Institute, University College Dublin, Belfield, Dublin D04 V1W8, Ireland. E-mail: brendan.kennedy@ucd.ie

**Received** 4 January 2017; **Revised** 26 April 2017; **Accepted** 15 May 2017

Stephanie L Merrigan and Breandán N Kennedy

*UCD School of Biomolecular and Biomedical Science, UCD Conway Institute, University College Dublin, Dublin, Ireland*

## BACKGROUND AND PURPOSE

Pathological growth of ocular vasculature networks can underpin visual impairment in neovascular age-related macular degeneration, proliferative diabetic retinopathy and retinopathy of prematurity. Our aim was to uncover novel pharmacological regulators of ocular angiogenesis by phenotype-based screening in zebrafish.

## EXPERIMENTAL APPROACH

A bioactive chemical library of 465 drugs was screened to identify small molecule inhibitors of ocular hyaloid vasculature (HV) angiogenesis in zebrafish larvae. Selectivity was assessed by evaluation of non-ocular intersegmental vasculature development. Safety pharmacology examined visual behaviour and retinal histology in larvae. Molecular mechanisms of action were scrutinized using expression profiling of target mRNAs and miRNAs in larval eyes.

## KEY RESULTS

Library screening identified 10 compounds which significantly inhibited HV developmental angiogenesis. The validated hit calcitriol selectively demonstrated dose-dependent attenuation of HV development. In agreement, vitamin D receptor (VDR) agonists paricalcitol, doxercalciferol, maxacalcitol, calcipotriol, seocalcitol, calcifediol and tacalcitol significantly and selectively attenuated HV development. VDR agonists induced minor ocular morphology abnormalities and affected normal visual function. Calcitriol induced a three to sevenfold increase in ocular dre-miR-21 expression. Consistently, all-trans-retinoic acid attenuated HV development and increased ocular dre-miR-21 expression. Interestingly, zebrafish ocular *vegfaa* and *vegfab* expression was significantly increased while, *vegfc, flt1* and *kdrl* expression was unchanged by calcitriol.

## CONCLUSION AND IMPLICATIONS

These studies identified VDR agonists as significant and selective anti-angiogenics in the developing vertebrate eye and miR21 as a key downstream regulated miRNA. These targets should be further evaluated as molecular hallmarks of, and therapeutic targets for pathological ocular neovascularization.

## Abbreviations

bp, base pair; calcitriol, 1,25-dihydroxyvitamin D3; CAM, chorioallantoic membrane; dpf, days post fertilization; *flt1*, fms-related tyrosine kinase 1; HIF-1α, hypoxia-inducible factor 1-α; hpf, hours post fertilization; HV, hyaloid vasculature; ISV, intersegmental vasculature; *kdrl*, kinase insert domain receptor like; nAMD, neovascular age-related macular degeneration; PDGFB, platelet derived growth factor B; PDR, proliferative diabetic retinopathy; PFA, paraformaldehyde; RA, all-*trans*-retinoic acid; RPE, retinal pigment epithelium; SPB, Sorenson's phosphate buffer; *Tg*(*fli1:*EGFP), Transgenic(*fli1*: EGFP); UCD, University College Dublin; VDR, vitamin D receptor; *vdra*, vitamin D receptor a; *vdrb*, vitamin D receptor b

DOI:10.1111/bph.13875

## Introduction

The eye requires a well-orchestrated vasculature supply to support the high metabolic demands of the photoreceptive retina (Wong-Riley, 2010). By adulthood, the human eye is perfused by two extensions of the ophthalmic artery, the choroidal and retinal vasculature systems (Hollyfield, 2011). The choroidal vasculature supports the anterior choroid, posterior choroid and outer retina. Large vessels of the Haller's layer, smaller vessels of Sattler's layer and the choriocapillaris adjacent to the Bruch's membrane collectively support photoreceptor function and waste elimination (Nickla and Wallman, 2010; Hollyfield, 2011; Branchini *et al.,* 2013; Zouache *et al.,* 2016). The inner retina is permeated and perfused by the retinal vasculature system, a system which protrudes through the posterior eye at the optic nerve head and branches into the ganglion cell layer, inner nuclear layer and marginally to the ora serrata (Fruttiger, 2007; Hollyfield, 2011). During human development, the inner retina is temporarily perfused by the hyaloid vasculature (HV) system, which regresses *in utero* together with retinal vasculogenesis (Hollyfield, 2011). This system enters the posterior of the eye as the vasa hyaloidea propia, branches throughout the primary optic vesicle towards the lens and attaches posteriorly and anteriorly as the tunica vasculosa lentis and the pupillary membrane respectively (Alvarez *et al.,* 2007; Fruttiger, 2007; Hollyfield, 2011). The HV system supports the retina during development and failure in its regression thereafter underpins visual impairment as persistent hyperplastic primary vitreous (Hollyfield, 2011).

Visual impairment can likewise result from dysregulated choroidal or retinal neovascularization. These are pathological hallmarks of leading causes of blindness worldwide, namely neovascular age-related macular degeneration (nAMD), retinopathy of prematurity and proliferative diabetic retinopathy (PDR) (Reynolds *et al.,* 2016). Late-stage nAMD manifests as a loss in central vision and is driven by pathological choroidal neovascularization. This pathological vasculature is deficient in tight junctions, projects through the Bruch's membrane and can cause retinal pigment epithelium (RPE) detachment (Campochiaro, 2013; Saint-Geniez and D'Amore, 2004). Current pharmacological interventions including Ranibizumab (Lucentis®; Genentech, Roche) and Aflibercept (Eylea®; Bayer, Regeneron) target aberrant vascularization though inhibition of the angiogenic factor **VEGF**. These interventions can decrease vision loss and improve visual acuity of nAMD patients; however, long-term studies with Ranibizumab report only one third of patients presenting with improved visual outcomes (Rofagha *et al.,* 2013). This limited efficacy, invasive route of intraocular administration and high economic burden underlines the need to identify alternative anti-angiogenics (Reynolds *et al.,* 2016).

Several studies document cellular and molecular mechanisms of pathological and developmental ocular vasculature growth. The retinal vasculature primarily forms via angiogenesis, a process of new vessels developing from pre-existing vasculature (Saint-Geniez and D'Amore, 2004). This tightly controlled cascade of events encompasses a pro-angiogenic switch in the endothelial cell micro-environment; pericyte detachment; budding vessel dilation; extracellular matrix remodelling; endothelial cell migration; tip cell selection; stalk elongation; tubule formation and vessel maturation (Carmeliet and Jain, 2011). Endogenous pro-angiogenic factors including VEGF, angiopoietin-1, angiopoietin-2, PDGF-A, PDGF-B and TGFβ as well as their cognate receptors promote vasculature development (Saint-Geniez and D'Amore, 2004). After development, a tightly regulated balance of pro- and anti-angiogenic factors maintains the mature vasculature. Pathological insults such as hypoxia can disrupt this equilibrium and promote angiogenesis (Folkman, 1995; Gariano and Gardner, 2005). For example, in PDR, pro-angiogenic growth factors, inflammatory cytokines and cells, vasoactive peptides and adhesion molecules are elevated in the vitreous and/or retina (Gariano and Gardner, 2005).

Here, we sought to identify pharmacological inhibitors of ocular developmental angiogenesis using a zebrafish model (Reynolds *et al.,* 2016). Similar to mammalian retinal and choroidal vasculature development, the zebrafish HV forms by angiogenesis (Hartsock *et al.,* 2014; Saint-Geniez and D'Amore, 2004). At early stages of zebrafish development, before 5 days post fertilization (dpf), this artery system passes through the choroid fissure and forms a network on the lens via tip cell driven hyaloid loop formation, network branching and pruning (Hartsock *et al.,* 2014). Late-stage HV development encompasses lens dissociation and transition to a retina-associated retinal vasculature network, without the HV regression seen in mammals (Alvarez *et al.,* 2007). The high fecundity, rapid embryonic development, optical transparency and availability of transgenic lines enable zebrafish to overcome the physiological simplicity of *in vitro* models and low-throughput of rodent models for pharmacological research (Chimote *et al.,* 2014). Over 65 small molecule screens using zebrafish to study phenotypic responses have been published (MacRae and Peterson, 2015). In this study, we coupled an established HV screening assay with the SCREEN-WELL® ICCB Known Bioactives library (Alvarez *et al.,* 2009; Reynolds *et al.,* 2016). Hit compounds, their pharmacological targets and their downstream signalling pathways can provide insights into developmental angiogenesis at a molecular level. Collectively, these can provide proof of principle encouraging hit to lead development of therapeutics for pathological neovascularization.

Here, unbiased screening of 465 bioactive library compounds identified 10 small molecule drugs that significantly inhibited HV developmental angiogenesis. Selected hit **1,25-dihydroxyvitamin D3** (calcitriol) and additional **vitamin D receptor** (VDR) agonists **paricalcitol**, **doxercalciferol**, **calcipotriol**, **seocalcitol**, **maxacalcitol**, **calcifediol** and **tacalcitol** were validated as attenuators of ocular vasculature development. VDR agonists induced no substantial reduction in developing or pre-developed non-ocular intersegmental vasculature (ISV), suggesting ocular-selective anti-angiogenic properties. Mechanistic evaluations show calcitriol-induced dre-miR-21 expression correlated with reduced ocular angiogenesis. Inhibitors of ocular angiogenesis, which act independently of VEGF attenuation, could act additively or synergistically with current interventions to treat pathological ocular neovascularization.

## Methods

### Zebrafish husbandry, randomization and ethical approval

Adult *Tg(fli1:*EGFP) zebrafish bred in the University College Dublin (UCD) Zebrafish Facility were maintained under recommended conditions specifically on a 14 h light and 10 h dark cycle at 28°C with brine-shrimp feeding twice daily (Matthews *et al.*, 2002). Embryos were acquired through natural spawning practices and maintained at 28°C in embryo medium filled petri dishes. Larvae were selected for experimentation based on morphological staging. Atypical larvae were omitted from studies and larvae randomly assigned to treatment groups. In addition, larvae within and across treatment groups originated from multiple stocks. Studies were conducted with approval exemption granted by the UCD Animal Research Ethics Committee (AREC-14-69, AREC-13-26 and AREC-14-68). Animal studies are reported in compliance with the ARRIVE guidelines (Kilkenny *et al.*, 2010; McGrath and Lilley, 2015).

### Chemical preparation

SCREEN-WELL® ICCB Known Bioactives library compounds supplied as 1, 0.1 mM or 5 mg·mL$^{-1}$ stocks were diluted to 100 μM working solutions in distilled water and stored at −20°C. Calcifediol (Selleckchem), doxercalciferol (Selleckchem), calcipotriol (Tocris), tacalcitol (Tocris), paricalcitol (Tocris), seocalcitol (Tocris), maxacalcitol (Cayman Chemical), calcitriol (Cayman Chemical) and **all-trans-retinoic acid** (RA; Sigma Aldrich) stocks were solubilized to 10 mM in DMSO and stored at −20 to −80°C. Further 100 μM working solutions in distilled water were prepared as required. Final dilutions and treatments were made in embryo medium.

### Phenotypic evaluation of ocular HV developmental angiogenesis

*Tg(fli1:*EGFP) zebrafish larvae received drug treatment at 2 dpf, by treatment of five larvae in each well of a 48-well plate with a final drug concentration of 0.1–10 μM in embryo medium. At 5 dpf, larvae were fixed overnight at 4°C in 4% paraformaldehyde (PFA) and subsequently washed in PBS. A single eye was enucleated from each fixed larva, the lens isolated and orientated allowing primary HV visualization by fluorescent microscopy (Olympus SZX16 fluorescence microscope and Cell^F software). The number of primary HV was manually quantified and representative images acquired. Library screening was performed in a blinded manner with access to drug lists granted after assessment of developmental angiogenesis.

### Phenotypic evaluation of trunk ISV developmental angiogenesis

*Tg(fli1:*EGFP) zebrafish larvae received drug treatment from 6–48 h post fertilization or 2–5 dpf. Treatments with five larvae in each well of a 48-well plate were performed with concentration of 10 or 20 μM in embryo medium. At 2 or 5 dpf, larvae were fixed overnight at 4°C in 4% PFA and washed in PBS. The number of ISV was quantified manually by fluorescent microscopy (Olympus SZX16 fluorescence microscope and Cell^F software) and representative images acquired.

### Phenotypic evaluation of overall gross morphology

*Tg(fli1:*EGFP) zebrafish larvae were treated and fixed as previously described from 2 to 5 dpf. Overall larval morphology was examined and the frequency of yolk sac and/or pericardial oedema quantified manually by brightfield microscopy (Olympus SZX16 -Cell^F software). Representative images were acquired.

### Zebrafish larval ocular histology

Larvae at 5 dpf were fixed overnight in 2.5% glutaraldehyde in 0.1 M Sorenson's phosphate buffer (SPB) (pH 7.3) at 4°C. Thereafter, larvae were washed with 0.1 M SPB and further fixed in 1% osmium tetroxide in 0.2 M SPB for 1 h. Before embedding, larvae were exposed to an ethanol gradient; 30, 50, 70 and 90% for 10 min each; 100% for 60 min and acetone for 30 min. Larvae were embedded in an epon resin composed of agar 100 resin; dodecenyl succinic anhydride; methyl nadic anhydride and 2,4,6-tris (dimethylaminomethyl) phenol overnight. Ultra-thin 1 μm ocular cross sections were obtained (Leica EM UC6 microtome), toluidine blue stained, cover-slipped (DPX mounting medium) and representative images acquired (Nikon Eclipse E80i Microscope, Canon camera). Sections were studied qualitatively for deviations in retinal lamination, cellular organization and morphological integrity compared with vehicle controls with treatments between 2 and 5 dpf.

### Zebrafish larval visual function assessment through optokinetic response evaluation

At 5 dpf, drug-treated larvae were washed with embryo medium, transferred individually to a 90 mm petri dish containing 9% methylcellulose and placed in a drum with black and white stripes (99% contrast and 18° per stripe). Larval optokinetic response was evaluated by manually counting the number of eye saccades per 60 s in response to both clockwise and counter-clockwise drum rotations at 18 rpm.

### Zebrafish total RNA extraction, cDNA synthesis and PCR

At 3, 4 or 5 dpf, larvae were stored in RNAlater (Qiagen), eyes enucleated and stored at 4°C in RNAlater. Total ocular RNA was extracted from ~60 pooled larvae using ThermoFisher Scientific mirVana™ miRNA Isolation Kit as per the manufacturer's instructions. Total RNA concentration was quantified at 260 nm (Spectrophotometer ND-1000) and samples stored at −80°C.

cDNA synthesis for *vdra, vdrb, vegfaa, vegfab, vegfc,* ***flt1****, kdrl* and 18S studies was carried out using Vilo system from Invitrogen as per the manufacturer's instructions. cDNA synthesis for dre-miR-21, dre-miR-150 and dre-miR-96 studies was carried out using TaqMan® MicroRNA Reverse Transcription Kit as per TaqMan® Small RNA Assays manufacturer's instructions.

RT-PCR reactions were made up on ice as per manufacturer's instruction using OneTaq® Quick-Load Master Mix

(NEB). Zebrafish *vdra* forward primer ACTCTCTGTCTGAC GCCTCT; zebrafish *vdra* reverse primer AGCGATCTGATCTT CAGCCG; zebrafish *vdrb* forward primer GTATGAAGCGG AAGGCCAGT; zebrafish *vdrb* reverse primer AACTGGAGG TCTGAAGCGTG. RT-PCR reactions were carried out under the following conditions: 95°C for 30 s (95°C for 30 s, 56°C for 30 s, 68°C for 1 min with 34 cycles) and 68°C for 5 min. RT-PCR products were run on a 1.5% agarose gel with 0.01% ethidium bromide (ThermoFisher Scientific) and bands compared with 50 base pair ladder (Invitrogen).

QRT-PCR reactions were made up on ice with 0.5 μL Taqman specific probe, 5 μL TaqMan Gene Expression Master Mix, 2.5 μL RNAse-free water and 2 μL cDNA template. QRT-PCR cycles were carried out with a 7900HT Fast Real-Time PCR system or QuantStudio 7 Flex Real-Time PCR System with SDS 2.4 Applied Biosystems or QuantStudio™ Software. The following conditions were applied: 50°C for 2 min, 95°C for 10 min, 95°C for 15 s with 40 repeats and 60°C for 1 min. Each of five biological assays was undertaken with two technical replicates and the average calculated for data analyses. dre-miR-21 and dre-miR-150 expression levels were normalized to dre-miR-96 (reference control). *vegfaa, vegfab, vegfc, flt1* and *kdrl* expression levels were normalized to 18S (reference control). Data presented as relative expression were analysed using the ΔΔCt method and fold change between vehicle control and treatment groups determined.

### Statistical analyses

Statistical difference between vehicle- and drug-treated groups was determined by one-way ANOVA with Dunnett's *post hoc* test or unpaired two-tailed *t*-test. Statistical analyses were performed with PRISM 5 software and significance was accepted where $P \leq 0.05$. The data and statistical analysis comply with the recommendations on experimental design and analysis in pharmacology (Curtis *et al.*, 2015).

### Nomenclature of targets and ligands

Key protein targets and ligands in this article are hyperlinked to corresponding entries in http://www.guidetopharmacology.org, the common portal for data from the IUPHAR/BPS Guide to PHARMACOLOGY (Southan *et al.*, 2016), and are permanently archived in the Concise Guide to PHARMACOLOGY 2015/16 (Alexander *et al.*, 2015a,b).

## Results

### Unbiased phenotype screening identified novel small molecule inhibitors of ocular developmental angiogenesis

To identify novel regulators of ocular angiogenesis, an unbiased phenotypic screen of the SCREEN-WELL® ICCB Known Bioactives library was undertaken in *Tg*(*fli1:*EGFP) zebrafish larvae. Compounds were screened for their ability to significantly reduce HV number between 2 and 5 dpf with 10 μM treatment (Figure 1A). Primary screening identified 20/465 compounds to attenuate HV developmental angiogenesis by >30% in *Tg*(*fli1:*EGFP) zebrafish larvae (Figure 1B). Lethality in 100% of treated larvae occurred with 44/465 compounds (data not shown). Secondary validation studies with 11 compounds, which attenuated HV development by ≥50%, confirmed the ability of primary hit compounds (10 μM) to reduce HV number.

The attenuation of HV development in larvae treated with **zaprinast**, a phosphodiesterase inhibitor; calcitriol, a VDR agonist; **forskolin**, an adenylate cyclase activator; **PP2**, an src family tyrosine kinase inhibitor; **FPL-64176**, a calcium channel ligand; trequinsin, a phosphodiesterase inhibitor; **vinpocetine**, a phosphodiesterase inhibitor; flunarizine-2HCl, a calcium channel ligand; **pimozide**, a calcium channel ligand; and penitrem A, a potassium channel ligand, was confirmed (Figure 1C). Calcitriol was selected for progression to efficacy, safety and mechanistic studies as the VDR pathway is known to inhibit tumour angiogenesis and low levels of vitamin D are a reported risk factor for nAMD (Chakraborti, 2011; Itty *et al.*, 2014). Calcitriol exerted a concentration-dependent reduction in HV developmental angiogenesis in *Tg*(*fli1:*EGFP) zebrafish larvae (Figure 1D, E). In agreement, RT-PCR confirms mRNA expression of the zebrafish VDR orthologues (*vdra* and *vdrb*) in larval eyes during the HV development window (Figure 1F).

### Vitamin D receptor agonists attenuate ocular developmental angiogenesis

To validate the specificity of the calcitriol response, the anti-angiogenic activity of seven commercially available VDR agonists was evaluated in *Tg*(*fli1:*EGFP) zebrafish larvae between 2 and 5 dpf. The VDR agonists, calcipotriol, seocalcitol and maxacalcitol, reported to present with improved safety profiles showed equivalent anti-angiogenic efficacy to calcitriol. The pre-hormone and circulating form of vitamin D, calcifediol, induced an anti-angiogenic response supporting the capability of its *in vivo* activation in zebrafish larvae. Vitamin $D_2$ analogues, paricalcitol and doxercalciferol, or vitamin $D_3$ analogue, tacalcitol, induced comparable 37 to 53% attenuation of ocular vasculature development compared with vehicle control (Figure 2A, B). Dose de-escalation studies evaluated the response of the vitamin $D_3$ analogue, tacalcitol or pre-hormone, calcifediol, which has lower VDR binding affinity or requires conversion to a more biological active form (Ritter and Brown, 2011). Significant reductions in HV development with 0.1–10 μM tacalcitol compared with 1–10 μM calcifediol were identified (Figure 2C, D).

### Vitamin D receptor agonists do not robustly attenuate trunk intersegmental vessel development

To evaluate the non-ocular anti-angiogenic effects of VDR agonists, trunk ISV number was quantified following drug treatment from 6 hpf to 2 dpf (Figure 3A). No significant reductions in ISV development were observed with 10 μM seocalcitol, maxacalcitol, calcitriol, calcifediol or tacalcitol treatment (data not shown), but 20 μM calcitriol and tacalcitol induced a modest (7–8%) yet significant reduction in ISV developmental angiogenesis in *Tg*(*fli1:*EGFP) zebrafish larvae (Figure 3C, E). Zebrafish larvae presented with no gross morphological defects, except for tacalcitol-treated larvae, which presented with reduced pigmentation and larval length, a phenotype suggestive of delayed development

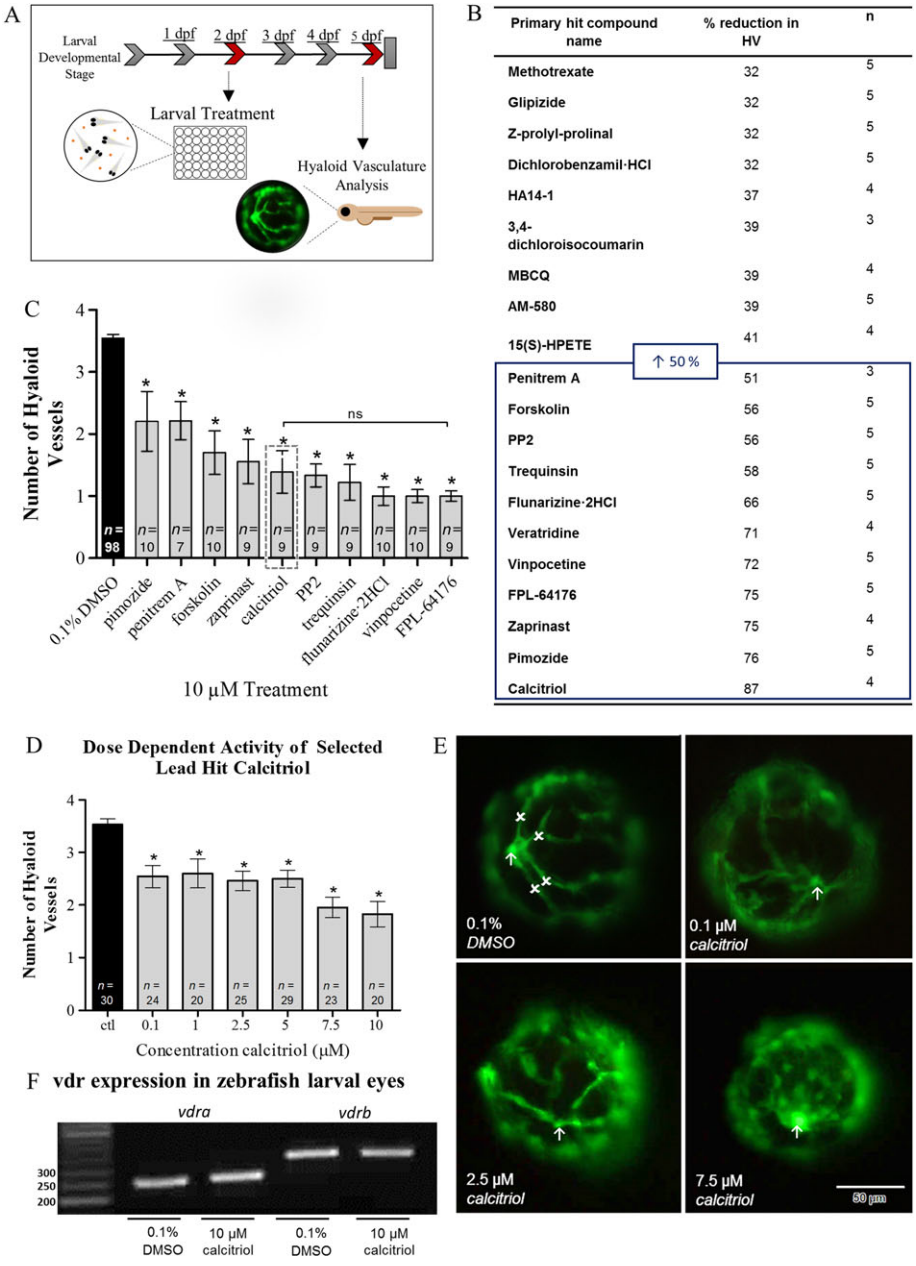


B

| Primary hit compound name | % reduction in HV | n |
|---|---|---|
| Methotrexate | 32 | 5 |
| Glipizide | 32 | 5 |
| Z-prolyl-prolinal | 32 | 5 |
| Dichlorobenzamil·HCl | 32 | 5 |
| HA14-1 | 37 | 4 |
| 3,4-dichloroisocoumarin | 39 | 3 |
| MBCQ | 39 | 4 |
| AM-580 | 39 | 5 |
| 15(S)-HPETE | 41 | 4 |
| ↑ 50 % | | |
| Penitrem A | 51 | 3 |
| Forskolin | 56 | 5 |
| PP2 | 56 | 5 |
| Trequinsin | 58 | 5 |
| Flunarizine·2HCl | 66 | 5 |
| Veratridine | 71 | 4 |
| Vinpocetine | 72 | 5 |
| FPL-64176 | 75 | 5 |
| Zaprinast | 75 | 4 |
| Pimozide | 76 | 5 |
| Calcitriol | 87 | 4 |

## Figure 1

A phenotype-based screen in zebrafish larvae identifies regulators of ocular HV developmental angiogenesis. (A) To identify novel regulators of ocular vessel growth, test compounds were screened for attenuation of ocular HV developmental angiogenesis in *Tg*(*fli1:*EGFP) zebrafish larvae. Pooled ($n = 5$) larvae were treated from 2 to 5 dpf and primary HV number subsequently quantified. (B) Table showing primary hit compounds from the SCREEN-WELL® ICCB Known Bioactives library screen, which were identified as regulators of zebrafish HV developmental angiogenesis. The table highlights compounds that reduced HV number by ≥32%. Compounds that inhibited HV development by ≥50%, were selected for secondary validation studies. (C) Bar chart representation of compounds found to attenuate HV developmental angiogenesis in primary and secondary screening. Graph showing mean ± SEM, one-way ANOVA with Dunnett's *post hoc* test analysis, asterisk signifies $P \leq 0.05$ and group size is indicated with *n* representing total number of larvae. Embryo lethality persisted with primary hit compound veratridine, and thus, further studies were not performed. Hit compound calcitriol was selected as lead hit, indicated by grey box. No significant (ns) difference in primary HV number was identified between calcitriol and FPL-64176, which presented with a marginally lower mean HV number. (D) Dose-dependent validation studies show calcitriol, 0.1–10 μM, to significantly attenuate HV number. Notably, the greatest inhibition of HV development was seen at concentrations ≥2.5 μM. Graph showing mean ± SEM, one-way ANOVA with Dunnett's *post hoc* test, asterisk signifies $P \leq 0.05$ and group size is indicated with *n* representing total number of larvae. (E) Qualitative representation of HV development at 5 dpf in response to 0.1% DMSO control or 0.1, 2.5 and 7.5 μM calcitriol treatment. Arrow indicates the optic nerve head, the point at which the HV emerges, and x highlights a primary HV branch. A clear diminution in HV number and vessel integrity can be seen in response to calcitriol treatment. Scale bar represents 50 μm. (F) The zebrafish *vdra* and *vdrb* mRNA is expressed in vehicle control and 10 μM calcitriol treated zebrafish larval eyes at 5 dpf. Representative RT-PCR gel, *vdra* product size: 254 base pair (bp) and *vdrb* product size: 320 bp. $n = 3$, where *n* represents pooled eyes isolated from 60 treated larvae.

A

| Compound | Chemical Structure | Biological Activity | % Reduction in HV | 10 μM Treatment |
|---|---|---|---|---|
| Paricalcitol | 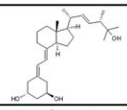 | *Tocris:* Analogue of the active form of vitamin D2 | 37 *n* = 23 | 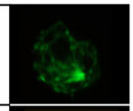 |
| Doxercalciferol | 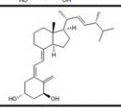 | *Selleckchem:* Synthetic vitamin D2 analogue | 41 *n* = 20 | 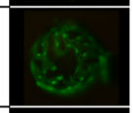 |
| Calcipotriol | 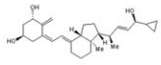 | *Tocris:* Vitamin D3 analogue with minimal effect on calcium homeostasis | 43 *n* = 26 | 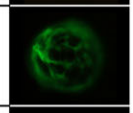 |
| Seocalcitol | 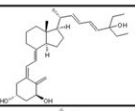 | *Tocris:* VDR agonist with reduced hypercalcemic effects. | 43 *n* = 27 | 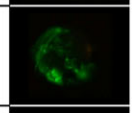 |
| Maxacalcitol | 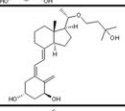 | *Cayman Chemical* Receptor-active form of vitamin D3, reported to avoid hypercalcemia. | 47 *n* = 26 | 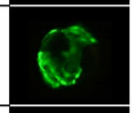 |
| Calcitriol | 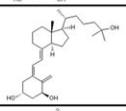 | *Cayman Chemical:* Screening hit 1α,25-dihydroxyitamin D3 | 48 *n* = 20 | 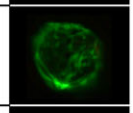 |
| Calcifediol | 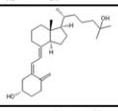 | *Selleckchem:* Major circulating metabolite of vitamin D3 | 50 *n* = 27 | 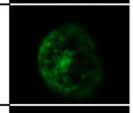 |
| Tacalcitol | 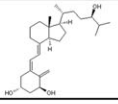 | *Tocris:* Synthetic vitamin D3 analogue | 53 *n* = 20 | 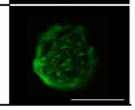 |

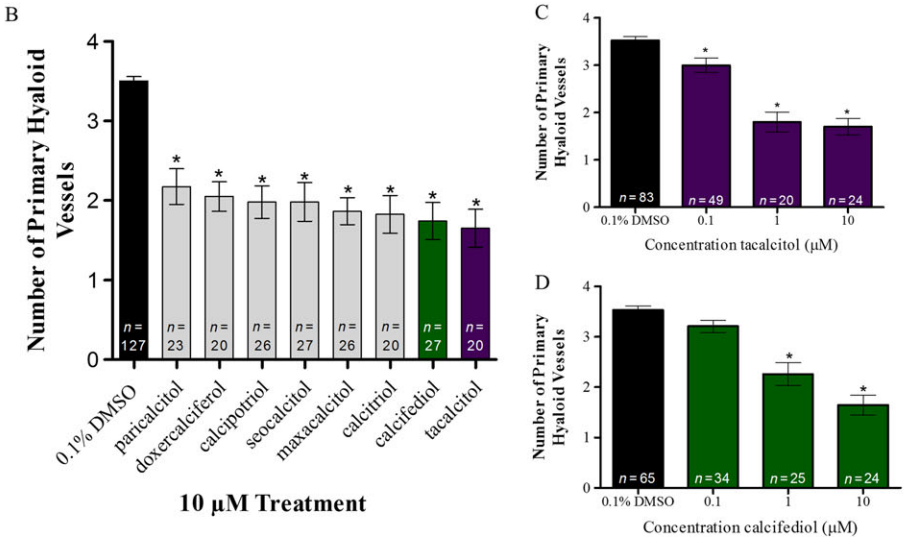


## Figure 2

VDR agonists attenuate developmental angiogenesis of ocular HV in zebrafish larvae. (A) Table giving the name, chemical structure, supplier pharmacological description, % reduction in zebrafish HV development at 5 dpf following 10 μM drug treatment from 2 dpf, group size with *n* representing total larvae and representative images of HV integrity at 5 dpf following drug treatment from 2 to 5 dpf. Scale bar represents 0.1 mm. (B) VDR agonists, paricalcitol, doxercalciferol, calcipotriol, seocalcitol, maxacalcitol, calcitriol, calcifediol (green) and tacalcitol (purple), reduce primary HV development between 2 and 5 dpf in zebrafish larvae. Graph showing mean ± SEM, one-way ANOVA with Dunnett's *post hoc* test analysis, asterisk signifies $P \leq 0.05$ and group size as indicated, with each *n* representing a single larva. (C) Dose de-escalation studies show tacalcitol (purple) significantly inhibits HV development in zebrafish larvae with 0.1–10 μM treatment. Graph showing mean ± SEM, one-way ANOVA with Dunnett's *post hoc* test analysis, asterisk signifies $P \leq 0.05$ and group size as indicated, with *n* representing total larvae. (D) Dose de-escalation studies show calcifediol (green) significantly inhibits HV development in zebrafish larvae with 1–10 μM treatment. Graph showing mean ± SEM, one-way ANOVA with Dunnett's *post hoc* test, asterisk signifies $P \leq 0.05$ and group size as indicated, with *n* representing total number of larvae.

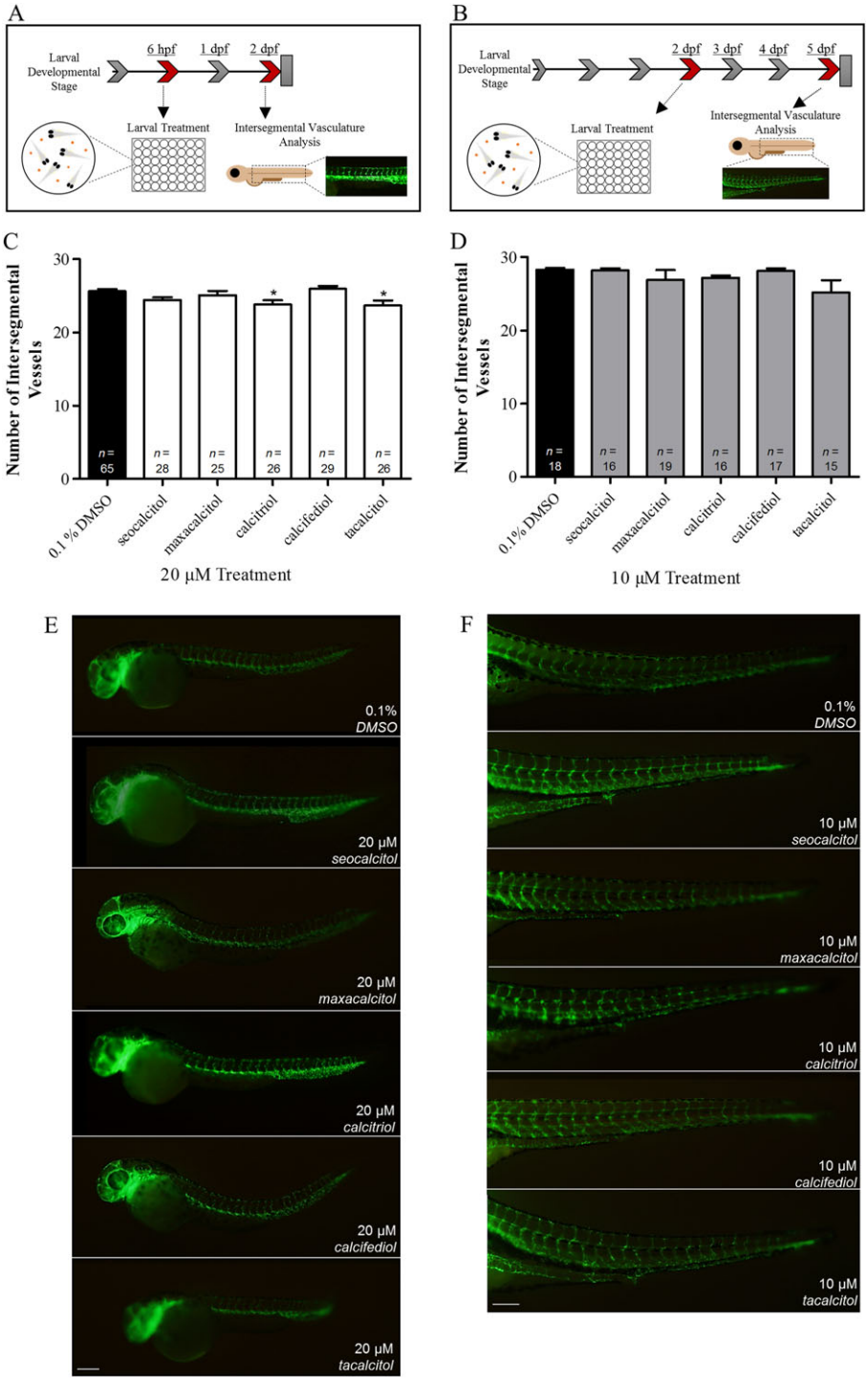


## Figure 3

Intersegmental vessel development and established intersegmental vessel integrity were not robustly affected by VDR agonist treatment. The effect of VDR agonist treatment on (A) ISV development between 6 hpf and 2 dpf and (B) ISV disruption between 2 and 5 dpf. (C) Treatment with 20 μM seocalcitol, maxacalcitol and calcifediol had no effect on ISV development, while calcitriol and tacalcitol significantly reduced development between 6 hpf and 2 dpf. Graph showing mean ± SEM, one-way ANOVA with Dunnett's *post hoc* test, asterisk signifies $P \leq 0.05$ and group size as indicated, with *n* representing total number of larvae. (D) Treatment with 10 μM seocalcitol, maxacalcitol, calcitriol, calcifediol and tacalcitol between 2 and 5 dpf had no effect on established ISV number. Graph showing mean ± SEM, one-way ANOVA with Dunnett's *post hoc* test analysis and group size as indicated, with *n* representing total number of larvae. (E) Qualitative representations of zebrafish larvae, showing ISV to be unchanged or slightly reduced in response to 20 μM seocalcitol, maxacalcitol, calcitriol, calcifediol and tacalcitol treatment between 6 hpf and 2 dpf. Scale bar represents 200 μm. (F) Qualitative representation of intact ISV after 10 μM seocalcitol, maxacalcitol, calcitriol, calcifediol and tacalcitol treatment from 2 to 5 dpf. Scale bar represents 200 μm.

(Figure 3E). To evaluate the effect of VDR agonist treatment on established vasculature, ISV number was quantified following drug treatment from 2 to 5 dpf (Figure 3B). VDR agonist treatments did not disrupt the number of established ISV in *Tg*(*fli1*:EGFP) zebrafish larvae (Figure 3D, F).

## *Vitamin D receptor agonist treatment adversely affects larvae visual response but not gross ocular histology*

We evaluated the ocular safety pharmacology of VDR agonists in zebrafish larvae by assessing visual function and ocular morphology. VDR agonists calcifediol, calcitriol, tacalcitol and maxacalcitol induced yolk sac and/or pericardial area oedema after treatment (2–5 dpf) in 55, 20, 50 or 40% of larvae respectively. In addition, 10 μM calcitriol induced 20% lethality before 5 dpf in treated larvae (Figure 4A, B). Assessment of visual function was conducted with the biologically active form of vitamin D, calcitriol. Calcitriol reduced larval optokinetic responses with several larvae exhibiting no visual response (Figure 4C). Ocular cross sections revealed the following: calcifediol to reduce eye size, increase numbers of pyknotic nuclei and affect retinal lamination; maxacalcitol to increase numbers of pyknotic nuclei; while tacalcitol and calcitriol to have no adverse effect on retinal patterning compared with vehicle control (Figure 4D).

## *Calcitriol significantly increases ocular dre-miR-21 expression from 3 dpf in zebrafish larvae*

miRNAs have a pivotal role in development and disease, tightly controlling processes including angiogenesis via post transcriptional regulation (Suarez and Sessa, 2009). Interestingly, Craig *et al.* (2014) revealed 31 miRNAs to be differentially regulated in whole zebrafish larvae in response to

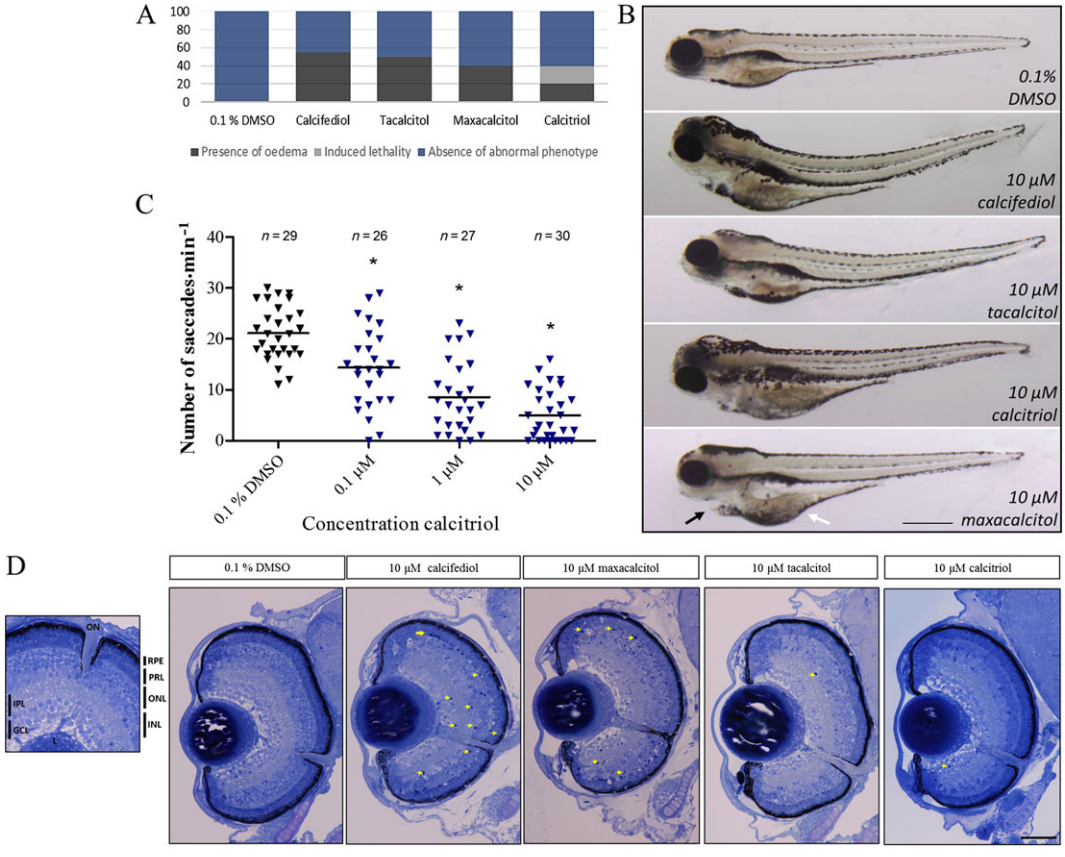


## Figure 4

VDR agonist treatment safety profile in zebrafish larvae. Zebrafish larval gross morphology, visual response and ocular histology after 10 μM VDR agonist treatment from 2 to 5 dpf. (A) Quantitative representation of the % of larvae exhibiting oedema after 10 μM VDR agonist treatment (dark grey stack). Oedema was seen in 55% of calcifediol; 20% of calcitriol; 50% of tacalcitol; and 40% of maxacalcitol-treated larvae. Notably, calcitriol induced lethality in 20% of treated larvae (light grey stack) ($n$ = 20). (B) Brightfield image representation of overall zebrafish larval morphology with 10 μM calcifediol, tacalcitol, maxacalcitol and calcitriol treatment. Larvae frequently presented with yolk sac (white arrow) and/or pericardial oedema (black arrow). Scale bar represents 500 μm. (C) A dose-dependent decline in larval visual response (optokinetic) was found with calcitriol treatment. Scatter plot showing saccades $min^{-1}$ per larva, one-way ANOVA with Dunnett's *post hoc* test, asterisk signifies $P \leq 0.05$, and group size as indicated, with $n$ representing total number of larvae. (D) Toluidine blue stained larval ocular cross sections show an absence of gross morphological defects and the presence of retinal lamination in VDR agonist-treated larvae between 2 and 5 dpf. Several larvae presented with pyknotic nuclei, indicated by yellow arrows ($n$ = 3). Scale bar represents 50 μm. PRL, photoreceptor layer; INL, inner nuclear layer; ONL, outer nuclear layer; IPL, inner plexiform layer; L, lens; GCL, ganglion cell layer.

calcitriol treatment. Here, dre-miR-21 and dre-miR-150 were selected for further analysis due to their previous link to ocular neovascularization (Wang *et al.,* 2012). Calcitriol treatment from 2 to 5 dpf induced no significant change in dre-miR-150 expression in zebrafish larval eyes (Figure 5B). In contrast, calcitriol treatment from 2 dpf significantly increased dre-miR-21 expression in zebrafish larval eyes at 3, 4 and 5 dpf (Figure 5C–E).

### *Calcitriol significantly increases ocular dre-miR-21 expression, a response mimicked with all-*trans*-retinoic acid treatment*

Calcitriol shares its heterodimerization partner retinoid X receptor with RA and notably calcitriol and RA induce synergistic anti-angiogenic activity (Majewski *et al.,* 1993; Jimenez-Lara and Aranda, 2000). Thus, the effect of RA treatment on zebrafish HV developmental angiogenesis, ocular dre-miR-21 expression and ocular dre-miR-150 expression was evaluated. RA treatments between 5 and 10 μM attenuate primary HV development in zebrafish larvae (Figure 6A, B). Akin to calcitriol, dre-miR-150 expression is unaltered, while dre-miR-21 expression was significantly up-regulated in eyes of larvae treated with an anti-angiogenic concentration of RA (Figure 6C, D).

### *Vitamin D receptor agonist treatment increases ocular vegfaa and vegfab expression in zebrafish larvae*

VEGF is known to have a crucial role in developmental and pathological angiogenesis. Here, we considered that VDR agonists may inhibit HV angiogenesis by reducing VEGF signalling. Interestingly, calcitriol treatment from 2 dpf significantly increased *vegfaa* expression in eyes isolated from larvae treated to 3, 4 or 5 dpf. A dose-dependent increase in *vegfaa* mRNA expression is observed in eyes with calcitriol treatment from 2 to 5 dpf, with statistical significance from 1 to 10 μM (Figure 7A). Calcitriol treatment from 2 dpf significantly increased *vegfab* expression in eyes isolated from larvae treated until 3 or 5 dpf, with a matching trend of increased expression at 4 dpf. Additionally, a dose-dependent increase in *vegfab* mRNA expression is observed in eyes subjected to calcitriol treatment from 2 to 5 dpf, with statistical significance at 1–10 μM (Figure 7B). No change in dre-miR-21 predicted target, *vegfc*, expression was seen in response to calcitriol treatment between 2–3, 2–4 and 2–5 dpf (Figure 7C). Zebrafish VEGF receptors *flt1* and *kdrl* also appear unchanged in response to calcitriol treatment (Figure 7D).

## Discussion

Angiogenesis is not only a key developmental process but also a pathological hallmark of ocular disease. Therefore, understanding the fundamental biology of angiogenesis could identify therapeutically tractable angiogenic pathways. Here, unbiased screening of the SCREEN-WELL® ICCB Known Bioactives library identified 10 drugs, including calcitriol, which significantly inhibit ocular developmental angiogenesis *in vivo*. Attenuation of ocular-specific angiogenesis was validated for all VDR agonists tested. Notably, this anti-angiogenic phenotype correlated with early augmentation of ocular dre-miR-21 expression. In agreement, RA, which similarly reduced ocular angiogenesis, also increased ocular dre-miR-21 expression. Collectively, this body of research positions VDR agonists and dre-miR-21 as key regulators of ocular developmental angiogenesis. In addition, although expression of *vegfc* and VEGF receptors appeared to be unaltered, ocular *vegfaa* and *vegfab* levels were significantly increased by calcitriol. This observation raises interest into the anti-angiogenic pathways downstream of VDR agonists.

Here, results from a Known Bioactives library screen using the established zebrafish HV assay are reported (Reynolds *et al.,* 2016). These library compounds have defined biological activities and targets. Therefore, hit compounds can (i) identify known molecular pathways with unforeseen significance in regulating ocular angiogenesis and (ii) unveil opportunities to reposition approved drugs for ocular indications. The anti-angiogenic hits validated here reveal consistencies and discrepancies with previous reports. For example, contrary to our findings, the phosphodiesterase inhibitor zaprinast promoted angiogenesis in the chicken chorioallantoic membrane (CAM) model (Pyriochou *et al.,* 2006) and the adenylate cyclase activator forskolin promoted angiogenesis *in vitro* and *in vivo* (Namkoong *et al.,* 2009). In agreement with our data, the src family tyrosine kinase inhibitor PP2 demonstrated robust anti-angiogenic activity in a rat model of pathological ocular angiogenesis (Werdich and Penn, 2006), and the phosphodiesterase inhibitors trequinsin and vinpocetine are linked to vasodilator activity and reduced vasculature remodelling respectively (Lal *et al.,* 1984; Cai *et al.,* 2012). Although no direct links between calcium channel regulators FPL-64176 or flunarizine and angiogenesis were identified, our findings are supported by prior reports of RPE cell dependence on calcium channels for pro-angiogenic VEGF secretion (Rosenthal *et al.,* 2007). Of particular interest was our discovery that the VDR agonist calcitriol produces a concentration-dependent inhibition of developmental angiogenesis in the zebrafish eye. This result is consistent with *in vitro* and *in vivo* evidence in chicken and rodent models; calcitriol significantly inhibits angiogenesis in the CAM model (Oikawa *et al.,* 1990), capillary network formation in mouse retinal endothelial cells and ocular neovascularization in an oxygen-induced retinopathy model (Albert *et al.,* 2007). Here, eight VDR agonists inhibited ocular angiogenesis, including three agonists with reduced hypercalcaemic profiles, suggesting this VDR activity is independent of high systemic calcium.

Calcitriol signalling through the nuclear VDR regulates over 900 genes in a micro-environment-specific manner (Alexander *et al.,* 2015a; Kongsbak *et al.,* 2013). In the human eye, the VDR is expressed in the, photoreceptors, RPE, lens, cornea, ganglion cell layer and ciliary body (Johnson *et al.,* 1995; Reins and McDermott, 2015). Expression of zebrafish VDR paralogues, *vdra* and *vdrb* arising from gene duplication, was validated here in larval eyes at 5 dpf by RT-PCR. Immunostaining previously reported VDR expression in zebrafish larvae, with localization to the retinal ganglion cells, parts of the brain and epithelial cells surrounding the otic vesicle (Craig *et al.,* 2008).

Interestingly, the established non-ocular vasculature of the trunk and tail was unaffected by VDR agonists,

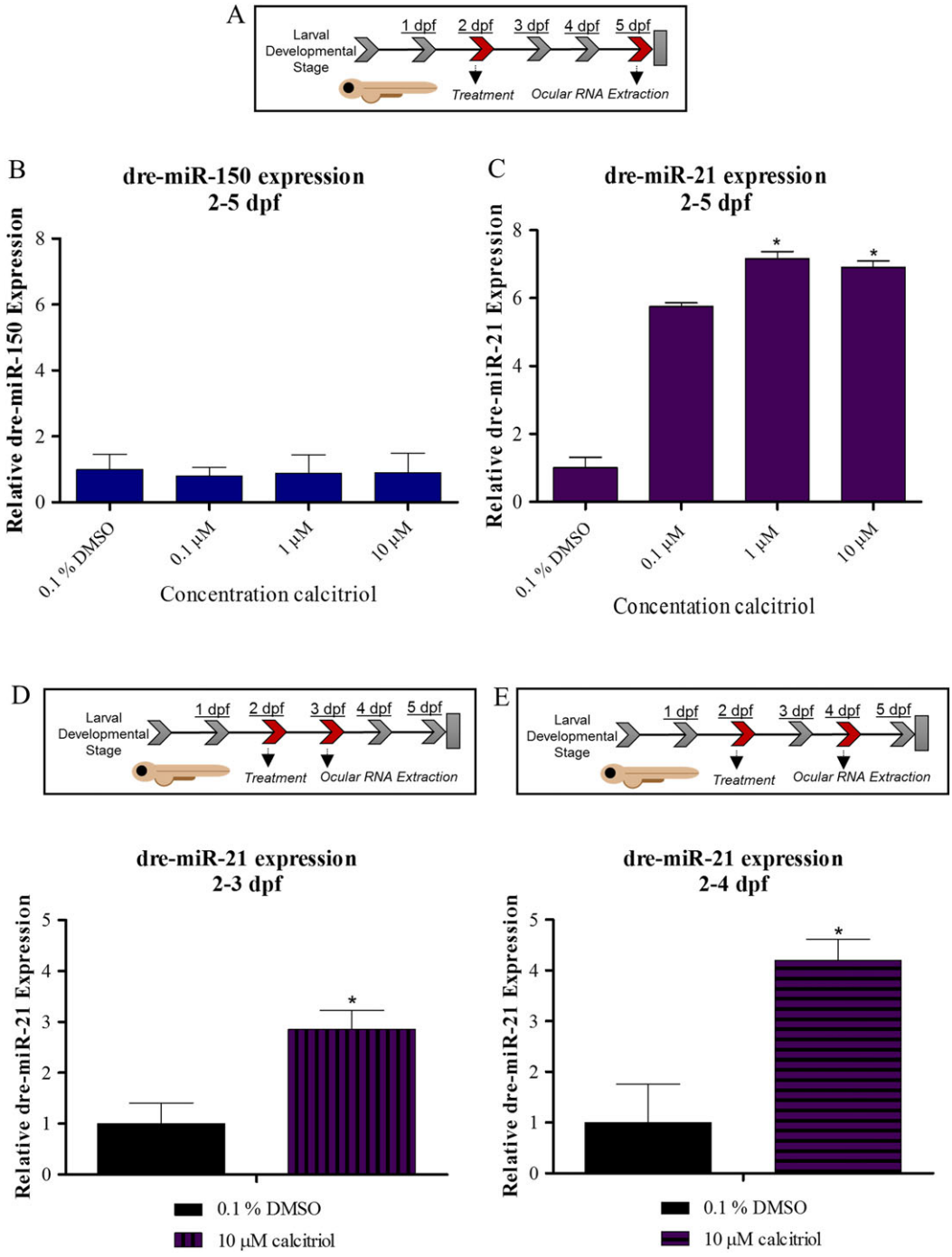


## Figure 5

Calcitriol regulates ocular dre-miR-21 expression in zebrafish larvae. (A) Expression of selected miRNA in zebrafish larval eyes was profiled following 0.1–10 μM calcitriol treatment from 2 to 5 dpf. (B) Ocular dre-miR-150 expression is unchanged by calcitriol treatment compared with 0.1% DMSO control. Graph showing mean fold change with ±SEM of treatment Ct, one-way ANOVA with Dunnett's *post hoc* test analysis and $n = 5$ with each $n$ representing eyes isolated from ~60 treated larvae. (C) Ocular dre-miR-21 expression is significantly up-regulated by calcitriol treatment compared with 0.1% DMSO control. Graph showing mean fold change with ±SEM of treatment Ct, one-way ANOVA with Dunnett's *post hoc* test analysis, asterisk denotes $P \leq 0.05$ and $n = 5$ with each $n$ representing eyes isolated from ~60 treated larvae. (D) Expression of dre-miR-21 in zebrafish larval eyes was profiled after 10 μM calcitriol treatment from 2 to 3 dpf. Ocular dre-miR-21 expression is significantly up-regulated by calcitriol treatment compared with 0.1% DMSO control. Graph showing mean fold change with ±SEM of treatment Ct, unpaired *t*-test analysis, asterisk denotes $P \leq 0.05$ and $n = 5$, with each $n$ representing eyes isolated from ~60 treated larvae. (E) Expression of dre-miR-21 in zebrafish larval eyes was profiled after 10 μM calcitriol treatment from 2 to 4 dpf. Ocular dre-miR-21 expression is significantly up-regulated by calcitriol treatment compared with 0.1% DMSO control. Graph showing mean fold change with ±SEM of treatment Ct, unpaired *t*-test analysis, asterisks denote $P \leq 0.05$ and $n = 5$ with each $n$ representing eyes isolated from ~60 treated larvae.

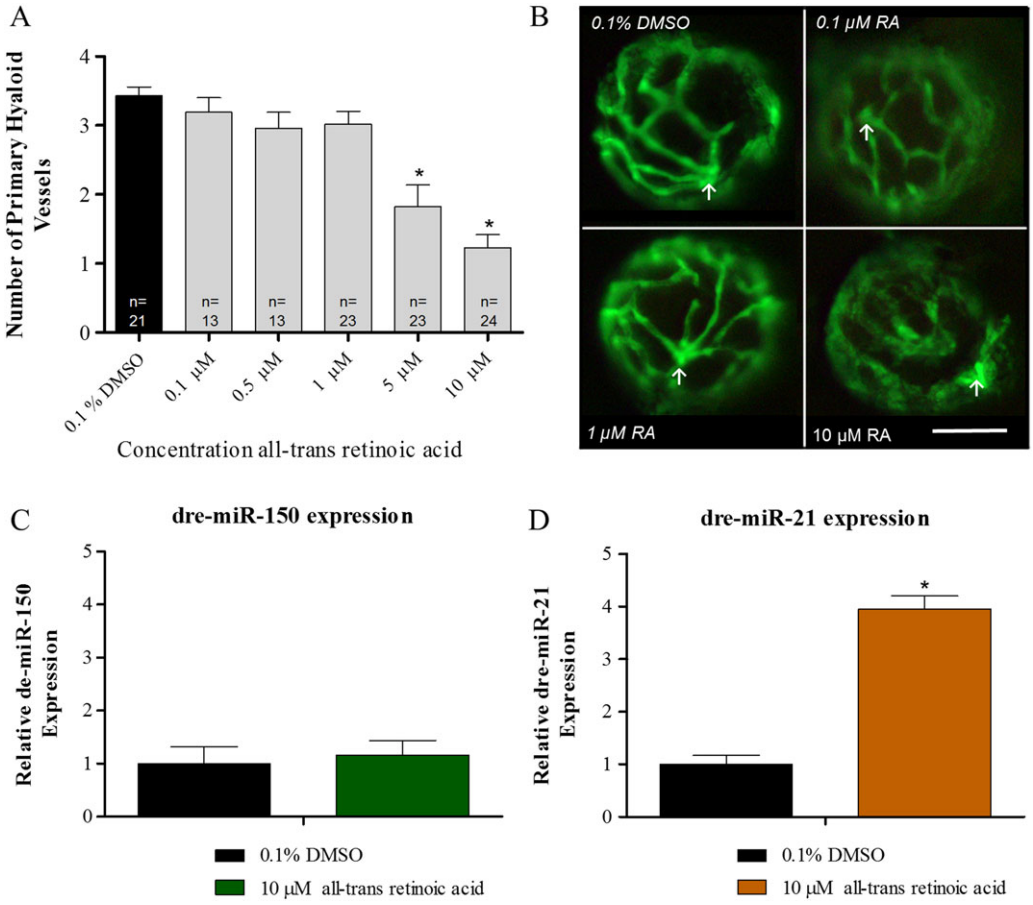


## Figure 6

All-*trans*-retinoic acid (RA) regulates ocular dre-miR-21 expression in zebrafish larvae. (A) RA significantly reduces HV angiogenesis in zebrafish larvae with treatments between 5 and 10 μM. Graph showing mean SEM, one-way ANOVA with Dunnett's *post hoc* test analysis, asterisk signifies $P \leq 0.05$ and group size as indicated, with *n* representing total larval number. (B) Phenotypic reduction in ocular HV development with 10 μM RA treatment compared with 0.1% DMSO control, 0.1 and 1 μM RA. Arrow indicates the optic nerve head, the point at which the HV emerges. A clear reduction in HV number and vessel integrity can be seen in response to 10 μM treatment. Scale bar represents 50 μm. (C) Ocular dre-miR-150 expression is unchanged by 10 μM RA treatment compared with 0.1% DMSO control. Graph showing mean fold change with ±SEM of treatment Ct, unpaired *t*-test analysis, $n = 5$ with each *n* representing eyes isolated from ~60 treated larvae. (D) Ocular dre-miR-21 expression is significantly up-regulated by 10 μM RA treatment compared with 0.1% DMSO control. Graph showing mean fold change with ±SEM of treatment Ct, unpaired *t*-test analysis, asterisks denote $P \leq 0.05$ and $n = 5$ with each *n* representing eyes isolated from ~60 treated larvae.

supporting anti-angiogenic, rather than vascular disrupting activity, in the eye (Ibrahim *et al.*, 2013). Pretreating embryos with VDR agonists before and during ISV development failed to induce an anti-angiogenic phenotype in these vessels, suggesting VDR agonists produce an ocular-selective inhibition of developmental angiogenesis. An equivalent ocular-specific anti-angiogenic response was reported with the PI3K inhibitor LY294002 (Alvarez *et al.*, 2009). This selectivity may reflect pharmacokinetic issues arising from the chorion acting as a physical barrier to drug absorption during embryonic development or the preferable absorption, distribution, metabolism and excretion properties of larval eyes (Sipes *et al.*, 2011). Notably, the small molecule anti-angiogenic quininib overcame these barriers and inhibited both HV and ISV development (Murphy *et al.*, 2016; Reynolds *et al.*, 2016).

In terms of initial ocular safety pharmacology, calcitriol-treated larvae presented with retinal morphology comparable with controls but poor visual function. This phenotype is consistent with loss of vasculature-derived signals that control retinal development, and we speculate that such adverse outcomes would not arise in a mature eye (Dhakal *et al.*, 2015). Indeed, apart from calcium deposits, severe adverse ocular effects are uncommon in adults with hypervitaminosis D (Fraunfelder *et al.*, 2014). Overall, the clinical use of calcitriol is limited by hypercalcaemia induced with therapeutically effective doses, thus analogues including maxacalcitol with reduced hypercalcaemia effects have been developed for indications such as psoriasis and secondary hyperparathyroidism (Brown and Slatopolsky, 2008).

Numerous studies propose *de novo* anti-angiogenic, anti-proliferative and pro-differentiation properties of VDR agonists (Chakraborti, 2011). However, downstream molecular pathways induced by VDR agonists are poorly defined. IL-8 secretion from human umbilical vein endothelial cells is attenuated by calcitriol (Bao *et al.*, 2006). MMP-2, MMP-9

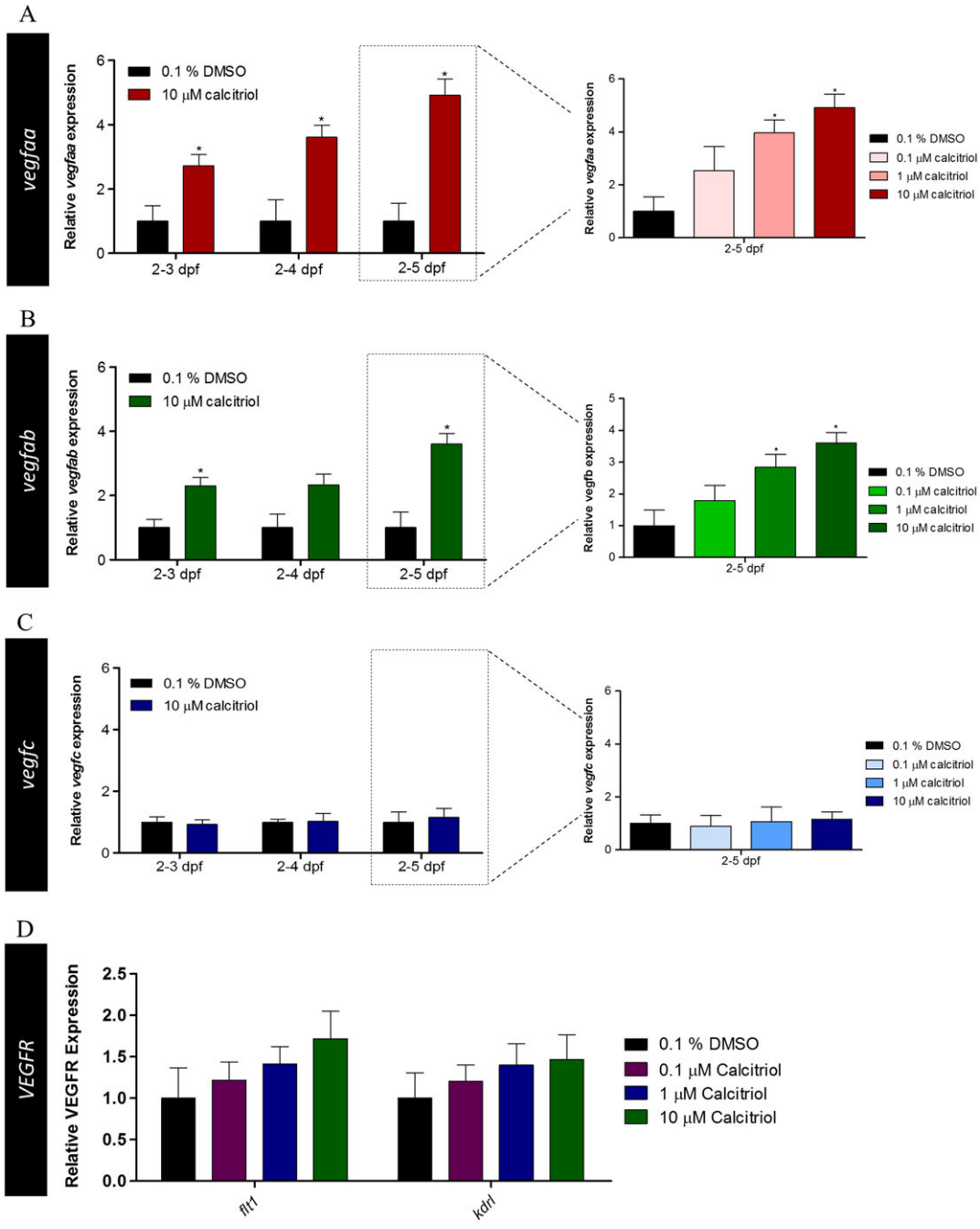


## Figure 7

Ocular VEGF and VEGF receptor expression in response to calcitriol treatment in zebrafish larvae. VEGF and VEGF receptor mRNA expression in the zebrafish larval eye was quantified after 0.1–10 μM calcitriol treatment between 2–3, 2–4 and 2–5 dpf. (A) *vegfaa* expression was significantly up-regulated in response to 10 μM calcitriol treatment between 2–3, 2–4 and 2–5 dpf. Dose de-escalation studies between 2 and 5 dpf showed 1–10 μM calcitriol treatment significantly up-regulated *vegfaa* expression, with no significant difference found at 0.1 μM. Graph showing mean fold change with ±SEM of treatment Ct, one-way ANOVA with Dunnett's *post hoc* test analysis, asterisk denotes $P \leq 0.05$ and $n = 5$ with each $n$ representing eyes isolated from ~60 treated larvae. (B) *vegfab* expression was significantly up-regulated in response to 10 μM calcitriol treatment between 2–3 and 2–5 dpf. Dose de-escalation studies between 2 and 5 dpf showed 1–10 μM calcitriol treatment significantly up-regulated *vegfab* expression, with no significant difference found at 0.1 μM. Graph showing mean fold change with ±SEM of treatment Ct, one-way ANOVA with Dunnett's *post hoc* test analysis, asterisk denotes $P \leq 0.05$ and $n = 5$ with each $n$ representing eyes isolated from ~60 treated larvae. (C) *vegfc* expression was unchanged by calcitriol treatment between 2–3, 2–4 and 2–5 dpf. Graph showing mean fold change with ±SEM of treatment Ct, one-way ANOVA with Dunnett's *post hoc* test analysis, asterisk denotes $P \leq 0.05$ and $n = 5$ with each $n$ representing eyes isolated from ~60 treated larvae. (D) No difference in the expression of the VEGF receptor, *flt1* and *kdrl*, was identified in response to 10 μM calcitriol treatment. Graph showing mean fold change with ±SEM of treatment Ct, one-way ANOVA with Dunnett's *post hoc* test analysis ($n = 5$; 0.1% DMSO and 10 μM calcitriol, $n = 3$; 0.1–1 μM calcitriol, with each $n$ representing eyes isolated from ~60 treated larvae).

and VEGF expression and secretion is reduced by VDR agonist treatment in Lewis lung carcinoma cells (Nakagawa *et al.*, 2005). Gene profiling shows an up-regulation of anti-angiogenic TGFβ, bone morphogenetic protein-2A and down-regulation of pro-angiogenic endothelin 1, cysteine-rich angiogenic inducer 61 and midkine by seocalcitol in human squamous carcinoma cells. Finally, in VDR null mice with tumour-induced angiogenesis, vessel enlargement reduced pericyte coverage, greater vasculature volume, vasculature leakage and up-regulation of pro-angiogenic factors VEGF, angiopoietin-1, PDGF-B and hypoxia-inducible factor 1-α (HIF-1α) result (Chung *et al.*, 2009).

Here, we uncovered a correlation between the anti-angiogenic efficacy of VDR agonists and increased miR21 expression in the eye. Nuclear receptors can regulate miRNA biogenesis and miRNA expression directly via promoter interaction or indirectly through an upstream target gene (Yang and Wang, 2011). Our data are consistent with previous reports demonstrating dre-miR-21 is regulated by calcitriol and that miR21 overexpression represses endothelial cell proliferation, migration, tubule formation and laser-induced choroidal neovascularization in mice (Sabatel *et al.*, 2011; Craig *et al.*, 2014). Furthermore, plasma miR21 expression is decreased in patients with nAMD (Ertekin *et al.*, 2014). Notably, miR-21 in the cancer field is an oncogene, which promotes angiogenesis, tumour growth and metastasis (Liu *et al.*, 2011). Here in contrast, increased dre-miR-21 expression correlated with reduced developmental angiogenesis. These contrasting results may be the consequence of site-specific regulation of gene expression, as miRNAs are capable of regulating up to 200 target genes (Carroll *et al.*, 2013). An equivalent paradigm is known for miR125b, which exhibits both oncogenic and tumour suppressive properties (Banzhaf-Strathmann and Edbauer, 2014). Elevated miR125b is linked to poor prognosis in colorectal cancer, with *in vitro* evidence supporting an attenuation of tumour suppressor

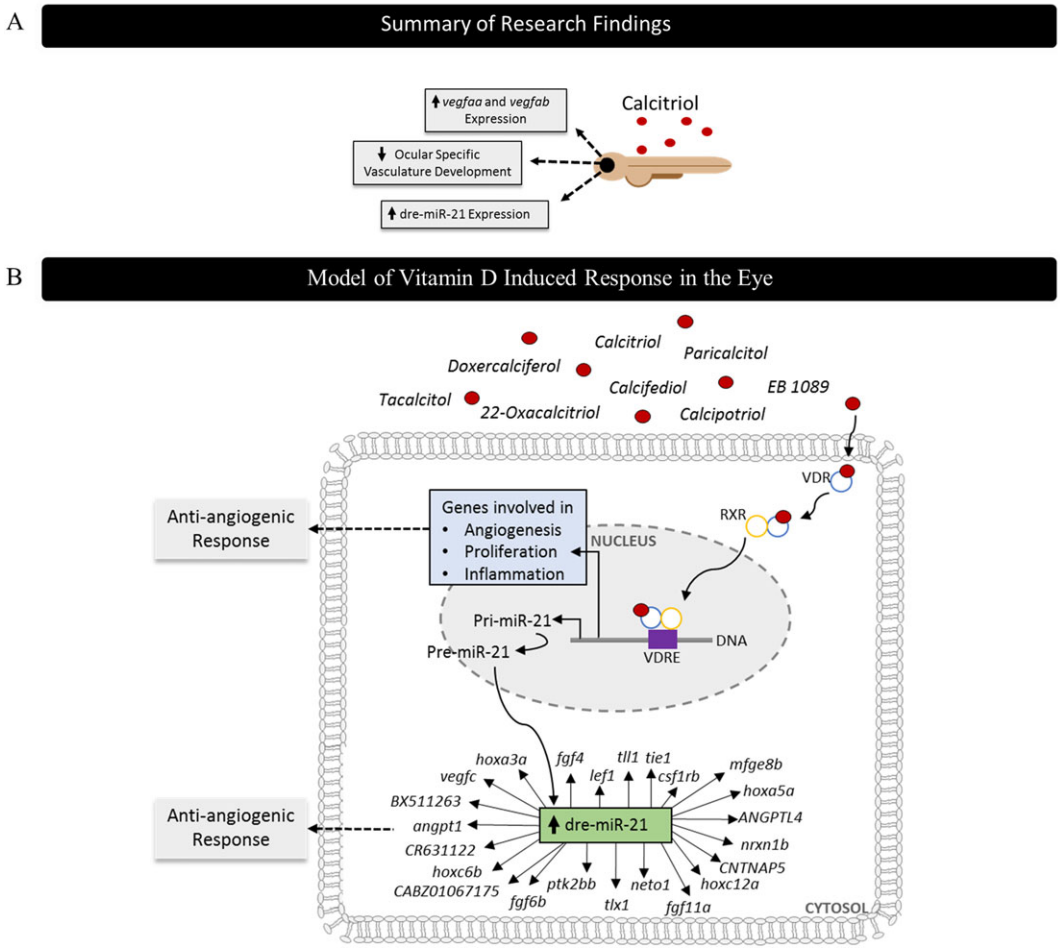


## Figure 8

Diagrammatic representation of key findings and prediction of anti-angiogenic mechanism of actions at a molecular level. (A) Zebrafish screening identified calcitriol as a regulator of developmental angiogenesis. Mechanistic insight found dre-miR-21, *vegfaa* and *vegfab* expression to be significantly up-regulated in response to calcitriol treatment. (B) Calcitriol traditionally mediates its effect through the VDR, and upon ligand interaction, it undergoes dimerisation with the retinoid X receptor (RXR), followed by binding to the vitamin D response element (VDRE) where it regulates gene expression. Here, we found an up-regulation of ocular dre-miR-21 with calcitriol treatments. Target prediction evaluation using TargetScanFish 6.2 predicted 3590 gene targets of dre-miR-21 and functional classification using Panther identified 23 genes to be linked to angiogenesis. Alternatively, the VDR may directly regulate genes involved in angiogenesis, proliferation, differentiation and inflammation.

gene p53 in response to miR125b (Nishida *et al.,* 2011). In contrast, miR125b expression is reduced in breast cancer and *in vitro* overexpression studies demonstrated tumour suppressor activity via mucin 1 repression (Rajabi *et al.,* 2010).

A previous report proposed vitamin D and retinoids to synergistically inhibit angiogenesis (Majewski *et al.,* 1996). Here, we showed that RA significantly attenuates ocular angiogenesis in zebrafish larvae, and interestingly, this also correlated with increased ocular dre-miR-21 expression. Together, these results further link dre-miR-21 augmentation to attenuated ocular angiogenesis.

VEGF promotes ocular vasculature growth through endothelial cell proliferation and migration, vessel patterning and tubule formation. Here, the dre-miR-21 predicted target *vegfc* expression was unaltered (Figure 8B), while an unexpected increase in *vegfaa* and *vegfab* expression was observed with calcitriol treatment. However, consistent with our data, miR21 was previously reported to increase VEGF expression in human prostate cancer via phosphatase and tensin homologue (PTEN) inhibition, resulting in Akt/ERK-mediated up-regulation of HIF-1α (Liu *et al.,* 2011). This unconventional response of an anti-angiogenic phenotype correlating with up-regulated VEGF may be the result of up-regulated VEGFxxxb, a VEGF-A splice variant, which negatively regulates angiogenesis (Nowak *et al.,* 2008). An isoform switch from predominately anti-angiogenic VEGFxxxb isoform to pro-angiogenic VEGFxxx isoform was identified in the vitreous of diabetic patients (Perrin *et al.,* 2005). Alternatively, increased VEGF expression could be a compensatory response to attenuated angiogenesis. Hypoxia following anti-VEGF treatment can induce expression of alternative pro-angiogenic growth factors, resulting in treatment resistance (Casanovas *et al.,* 2005). Overall, the time- and dose-dependent results presented here support an anti-angiogenic mechanism independent of attenuated VEGF in the zebrafish eye. However, further studies incorporating gene knockouts and investigating biochemical changes at the protein level are required to validate the requirement of VDR, VEGF and miR21 orthologues for this response.

In conclusion, our results validate the anti-angiogenic activity of VDR agonists. We showed for the first time the ability of calcitriol and other VDR agonists to significantly and selectively inhibit developmental angiogenesis in the zebrafish larval eye. This anti-angiogenic phenotype correlates with increased ocular dre-miR-21 expression. Interestingly, this response was independent of targeted inhibition of VEGF, the mechanism of clinically approved ocular anti-angiogenics (Figure 8). VDR signalling represents a target of interest for the prevention and treatment of ocular angiogenic disorders.

## Acknowledgements

We thank Catherine Moss of the UCD Conway Institute genomics facility for assistance with QRT-PCR data analyses and use of facility. We thank the staff of the UCD Conway Institute imaging facility for technical support. We thank Dr Yolanda Alvarez and Dr Alison Reynolds for manuscript proof reading. This work was supported by the Health Research Board, HRB-POR-2013-390, and the Irish Research Council, GOIPG/2015/2061.

## Author contributions

Experiments, data analyses and manuscript writing were performed by S.L.M. Supervision, resources, experimental design, results interpretation and manuscript writing were carried out by B.N.K.

## Conflict of interest

The authors declare no conflicts of interest.

## Declaration of transparency and scientific rigour

This Declaration acknowledges that this paper adheres to the principles for transparent reporting and scientific rigour of preclinical research recommended by funding agencies, publishers and other organisations engaged with supporting research.

## References

Albert DM, Scheef EA, Wang S, Mehraein F, Darjatmoko SR, Sorenson CM *et al.* (2007). Calcitriol is a potent inhibitor of retinal neovascularization. Invest Ophthalmol Vis Sci 48: 2327–2334.

Alexander SPH, Cidlowski JA, Kelly E, Marrion N, Peters JA, Benson HE *et al.* (2015a). The Concise Guide to PHARMACOLOGY 2015/16: Nuclear hormone receptors. Br J Pharmacol 172: 5956–5978.

Alexander SPH, Fabbro D, Kelly E, Marrion N, Peters JA, Benson HE *et al.* (2015b). The Concise Guide to PHARMACOLOGY 2015/16: Catalytic receptors. Br J Pharmacol 172: 5979–6023.

Alvarez Y, Astudillo O, Jensen L, Reynolds AL, Waghorne N, Brazil DP *et al.* (2009). Selective inhibition of retinal angiogenesis by targeting PI3 kinase. PloS one 4: e7867.

Alvarez Y, Cederlund ML, Cottell DC, Bill BR, Ekker SC, Torres-Vazquez J *et al.* (2007). Genetic determinants of hyaloid and retinal vasculature in zebrafish. BMC Dev Biol 7: 114.

Banzhaf-Strathmann J, Edbauer D (2014). Good guy or bad guy: the opposing roles of microRNA 125b in cancer. Cell Commun Signal 12: 30.

Bao BY, Yao J, Lee YF (2006). 1alpha, 25-dihydroxyvitamin D3 suppresses interleukin-8-mediated prostate cancer cell angiogenesis. Carcinogenesis 27: 1883–1893.

Branchini LA, Adhi M, Regatieri CV, Nandakumar N, Liu JJ, Laver N *et al.* (2013). Analysis of choroidal morphologic features and vasculature in healthy eyes using spectral-domain optical coherence tomography. Ophthalmology 120: 1901–1908.

Brown AJ, Slatopolsky E (2008). Vitamin D analogs: therapeutic applications and mechanisms for selectivity. Mol Aspects Med 29: 433–452.

Cai Y, Knight WE, Guo S, Li JD, Knight PA, Yan C (2012). Vinpocetine suppresses pathological vascular remodeling by inhibiting vascular smooth muscle cell proliferation and migration. J Pharmacol Exp Ther 343: 479–488.

Campochiaro PA (2013). Ocular neovascularization. J Mol Med (Berlin, Germany) 91: 311–321.

Carmeliet P, Jain RK (2011). Molecular mechanisms and clinical applications of angiogenesis. Nature 473: 298–307.

Carroll AP, Tooney PA, Cairns MJ (2013). Context-specific microRNA function in developmental complexity. J Mol Cell Biol 5: 73–84.

Casanovas O, Hicklin DJ, Bergers G, Hanahan D (2005). Drug resistance by evasion of antiangiogenic targeting of VEGF signaling in late-stage pancreatic islet tumors. Cancer Cell 8: 299–309.

Chakraborti CK (2011). Vitamin D as a promising anticancer agent. Indian J Pharmacol 43: 113–120.

Chimote G, Sreenivasan J, Pawar N, Subramanian J, Sivaramakrishnan H, Sharma S (2014). Comparison of effects of anti-angiogenic agents in the zebrafish efficacy-toxicity model for translational anti-angiogenic drug discovery. Drug Des Devel Ther 8: 1107–1123.

Chung I, Han G, Seshadri M, Gillard BM, Yu WD, Foster BA *et al.* (2009). Role of vitamin D receptor in the antiproliferative effects of calcitriol in tumor-derived endothelial cells and tumor angiogenesis in vivo. Cancer Res 69: 967–975.

Craig TA, Sommer S, Sussman CR, Grande JP, Kumar R (2008). Expression and regulation of the vitamin D receptor in the zebrafish, Danio rerio. J Bone Miner Res 23: 1486–1496.

Craig TA, Zhang Y, Magis AT, Funk CC, Price ND, Ekker SC *et al.* (2014). Detection of 1alpha,25-dihydroxyvitamin D-regulated miRNAs in zebrafish by whole transcriptome sequencing. Zebrafish 11: 207–218.

Curtis MJ, Bond RA, Spina D, Ahluwalia A, Alexander SP, Giembycz MA *et al.* (2015). Experimental design and analysis and their reporting: new guidance for publication in BJP. Br J Pharmacol 172: 3461–3471.

Dhakal S, Stevens CB, Sebbagh M, Weiss O, Frey RA, Adamson S *et al.* (2015). Abnormal retinal development in Cloche mutant zebrafish. Dev Dyn 244: 1439–1455.

Ertekin S, Yildirim O, Dinc E, Ayaz L, Fidanci SB, Tamer L (2014). Evaluation of circulating miRNAs in wet age-related macular degeneration. Mol Vis 20: 1057–1066.

Folkman J (1995). Angiogenesis in cancer, vascular, rheumatoid and other disease. Nat Med 1: 27–31.

Fraunfelder FT, Fraunfelder FW, Chambers WA (2014). Drug-Induced Ocular Side Effects: Clinical Ocular Toxicology E-Book. Elsevier Health Sciences.

Fruttiger M (2007). Development of the retinal vasculature. Angiogenesis 10: 77–88.

Gariano RF, Gardner TW (2005). Retinal angiogenesis in development and disease. Nature 438: 960–966.

Hartsock A, Lee C, Arnold V, Gross JM (2014). In vivo analysis of hyaloid vasculature morphogenesis in zebrafish: a role for the lens in maturation and maintenance of the hyaloid. Dev Biol 394: 327–339.

Hollyfield BA-AJG (2011). The Retina and Its Disorders. Academic Press: The Boulevard, Langford Lane, Kidlington, Oxford OX5 1GB, UK. Available at: https://www.elsevier.com/books/the-retina-and-its-disorders/besharse/978-0-12-382198-0.

Ibrahim MA, Do DV, Sepah YJ, Shah SM, Van Anden E, Hafiz G *et al.* (2013). Vascular disrupting agent for neovascular age related macular degeneration: a pilot study of the safety and efficacy of intravenous combretastatin A-4 phosphate. BMC Pharmacol Toxicol 14: 7.

Itty S, Day S, Lyles KW, Stinnett SS, Vajzovic LM, Mruthyunjaya P (2014). Vitamin D deficiency in neovascular versus nonneovascular age-related macular degeneration. Retina (Philadelphia, Pa) 34: 1779–1786.

Jimenez-Lara AM, Aranda A (2000). Interaction of vitamin D and retinoid receptors on regulation of gene expression. Horm Res 54: 301–305.

Johnson JA, Grande JP, Roche PC, Campbell RJ, Kumar R (1995). Immuno-localization of the calcitriol receptor, calbindin-D28k and the plasma membrane calcium pump in the human eye. Curr Eye Res 14: 101–108.

Kilkenny C, Browne W, Cuthill IC, Emerson M, Altman DG (2010). Animal research: reporting in vivo experiments: the ARRIVE guidelines. Br J Pharmacol 160: 1577–1579.

Kongsbak M, Levring TB, Geisler C, von Essen MR (2013). The vitamin d receptor and T cell function. Front Immunol 4: 148.

Lal B, Dohadwalla AN, Dadkar NK, D'Sa A, de Souza NJ (1984). Trequinsin, a potent new antihypertensive vasodilator in the series of 2-(arylimino)-3-alkyl-9,10-dimethoxy-3,4,6,7-tetrahydro-2H-py rim ido [6,1-a]isoquinolin-4-ones. J Med Chem 27: 1470–1480.

Liu LZ, Li C, Chen Q, Jing Y, Carpenter R, Jiang Y *et al.* (2011). MiR-21 induced angiogenesis through AKT and ERK activation and HIF-1alpha expression. PloS one 6: e19139.

MacRae CA, Peterson RT (2015). Zebrafish as tools for drug discovery. Nat Rev Drug Discov 14: 721–731.

Majewski S, Skopinska M, Marczak M, Szmurlo A, Bollag W, Jablonska S (1996). Vitamin D3 is a potent inhibitor of tumor cell-induced angiogenesis. J Investig Dermatol Symp Proc 1: 97–101.

Majewski S, Szmurlo A, Marczak M, Jablonska S, Bollag W (1993). Inhibition of tumor cell-induced angiogenesis by retinoids, 1,25-dihydroxyvitamin D3 and their combination. Cancer Lett 75: 35–39.

Matthews M, Trevarrow B, Matthews J (2002). A virtual tour of the guide for zebrafish users. Lab Anim 31: 34–40.

McGrath JC, Lilley E (2015). Implementing guidelines on reporting research using animals (ARRIVE etc.): new requirements for publication in BJP. Br J Pharmacol 172: 3189–3193.

Murphy AG, Casey R, Maguire A, Tosetto M, Butler CT, Conroy E *et al.* (2016). Preclinical validation of the small molecule drug quininib as a novel therapeutic for colorectal cancer. Sci Rep 6: 34523.

Nakagawa K, Sasaki Y, Kato S, Kubodera N, Okano T (2005). 22-Oxa-1alpha,25-dihydroxyvitamin D3 inhibits metastasis and angiogenesis in lung cancer. Carcinogenesis 26: 1044–1054.

Namkoong S, Kim CK, Cho YL, Kim JH, Lee H, Ha KS *et al.* (2009). Forskolin increases angiogenesis through the coordinated cross-talk of PKA-dependent VEGF expression and Epac-mediated PI3K/Akt/eNOS signaling. Cell Signal 21: 906–915.

Nickla DL, Wallman J (2010). The multifunctional choroid. Prog Retin Eye Res 29: 144–168.

Nishida N, Yokobori T, Mimori K, Sudo T, Tanaka F, Shibata K *et al.* (2011). MicroRNA miR-125b is a prognostic marker in human colorectal cancer. Int J Oncol 38: 1437–1443.

Nowak DG, Woolard J, Amin EM, Konopatskaya O, Saleem MA, Churchill AJ *et al.* (2008). Expression of pro- and anti-angiogenic isoforms of VEGF is differentially regulated by splicing and growth factors. J Cell Sci 121: 3487–3495.

Oikawa T, Hirotani K, Ogasawara H, Katayama T, Nakamura O, Iwaguchi T*et al.* (1990). Inhibition of angiogenesis by vitamin D3 analogues. Eur J Pharmacol 178: 247–250.

Perrin RM, Konopatskaya O, Qiu Y, Harper S, Bates DO, Churchill AJ (2005). Diabetic retinopathy is associated with a switch in splicing from anti- to pro-angiogenic isoforms of vascular endothelial growth factor. Diabetologia 48: 2422–2427.

Pyriochou A, Beis D, Koika V, Potytarchou C, Papadimitriou E, Zhou Z *et al.* (2006). Soluble guanylyl cyclase activation promotes angiogenesis. J Pharmacol Exp Ther 319: 663–671.

Rajabi H, Jin C, Ahmad R, McClary C, Joshi MD, Kufe D (2010). Mucin 1 oncoprotein expression is suppressed by the miR-125b oncomir. Genes & cancer 1: 62–68.

Reins RY, McDermott AM (2015). Vitamin D: implications for ocular disease and therapeutic potential. Exp Eye Res 134: 101–110.

Reynolds AL, Alvarez Y, Sasore T, Waghorne N, Butler CT, Kilty C *et al.* (2016). Phenotype-based discovery of 2-[(E)-2-(quinolin-2-yl) vinyl]phenol as a novel regulator of ocular angiogenesis. J Biol Chem 291: 7242–7255.

Ritter CS, Brown AJ (2011). Direct suppression of Pth gene expression by the vitamin D prohormones doxercalciferol and calcidiol requires the vitamin D receptor. J Mol Endocrinol 46: 63–66.

Rofagha S, Bhisitkul RB, Boyer DS, Sadda SR, Zhang K (2013). Seven-year outcomes in ranibizumab-treated patients in ANCHOR, MARINA, and HORIZON: a multicenter cohort study (SEVEN-UP). Ophthalmology 120: 2292–2299.

Rosenthal R, Heimann H, Agostini H, Martin G, Hansen LL, Strauss O (2007). Ca2+ channels in retinal pigment epithelial cells regulate vascular endothelial growth factor secretion rates in health and disease. Mol Vis 13: 443–456.

Sabatel C, Malvaux L, Bovy N, Deroanne C, Lambert V, Gonzalez ML *et al.* (2011). MicroRNA-21 exhibits antiangiogenic function by targeting RhoB expression in endothelial cells. PloS one 6: e16979.

Saint-Geniez M, D'Amore PA (2004). Development and pathology of the hyaloid, choroidal and retinal vasculature. Int J Dev Biol 48: 1045–1058.

Sipes NS, Padilla S, Knudsen TB (2011). Zebrafish: as an integrative model for twenty-first century toxicity testing. Birth Defects Res C, Embryo Today 93: 256–267.

Southan C, Sharman JL, Benson HE, Faccenda E, Pawson AJ, Alexander SP *et al.* (2016). The IUPHAR/BPS guide to PHARMACOLOGY in 2016: towards curated quantitative interactions between 1300 protein targets and 6000 ligands. Nucl Acids Res 44: D1054–D1068.

Suarez Y, Sessa WC (2009). MicroRNAs as novel regulators of angiogenesis. Circ Res 104: 442–454.

Wang S, Koster KM, He Y, Zhou Q (2012). miRNAs as potential therapeutic targets for age-related macular degeneration. Future Med Chem 4: 277–287.

Werdich XQ, Penn JS (2006). Specific involvement of SRC family kinase activation in the pathogenesis of retinal neovascularization. Invest Ophthalmol Vis Sci 47: 5047–5056.

Wong-Riley MT (2010). Energy metabolism of the visual system. Eye Brain 2: 99–116.

Yang Z, Wang L (2011). Regulation of microRNA expression and function by nuclear receptor signaling. Cell & bioscience 1: 31.

Zouache MA, Eames I, Klettner CA, Luthert PJ (2016). Form, shape and function: segmented blood flow in the choriocapillaris. Scientific reports 6: 35754.